2022 19th International Conference on Electrical Engineering, Computing Science and Automatic Control (CCE)
Mexico City, Mexico. November 9-11, 2022

# On the validation of an acoustic black hole in Euler-Bernoulli beams: experimental results

Jorge Ivan Valdes-Ceron
*Centro de Investigacion y de Estudios Avanzados del I.P.N*
*Department of Electrical Engineering, Mechatronics Section*
CDMX, Mexico
ivan.valdes@cinvestav.mx

Gerardo Silva-Navarro
*Centro de Investigacion y de Estudios Avanzados del I.P.N*
*Department of Electrical Engineering, Mechatronics Section*
CDMX, Mexico
gsilva@cinvestav.mx

***Abstract*—This work addresses an experimental validation of acoustic black holes in Euler-Bernoulli beams to evaluate its potential application as passive vibration absorbers on mechanical structures. The experimental validation was performed in two different ways, the first based on acceleration and the second on audio measurements. The experimental results can validate the vibration absorption capability using a low-cost method based on acoustic measurements and modal analysis techniques.**

***Keywords*—Acoustic black hole, Mechanical vibrations, Modal analysis, Passive vibration absorbers.**

## I. Introduction

Acoustic Black Holes (ABH) are mechanical devices capable of concentrating mechanical vibrations due to the interface that they form with an elastic medium [1,2]. There are several types of geometries with ABH analyzed in the literature, although the case of beam has been more extensive [2,3].

The physical principle of the ABH occurs in the field of propagation of mechanical waves in elastic media, where the ABH forms an interface that will allow the travelling of waves of certain frequencies and then, due to the variable decrease in the thickness of a beam, these flexural waves are carried to a wave speed close to zero, where the phase of the wave tends to infinity and, therefore, the waves are confined to the tip of the ABH, where the structural damping of the material can dissipate them [2,3].

In practice, however, the theoretical phenomenon does not perfectly occur, mainly because there are physical imperfections in the profiles or the truncation of the ABH tip. Physically it is not possible to have zero thickness at the tip, although in the literature there are some results improving the ideal performance, despite such defects, by incorporating layers of viscoelastic materials that allow quick energy dissipation as soon as they reach the tip, before their return [2,3]. This work considers Euler-Bernoulli beams with variable (thickness) cross section, starting with the fundamental background, description of the case study, modal analysis, and concluding with numerical and experimental validations.

## II. A Brief Review of ABH Applications

The ABHs have deserved attention during the last two decades. Most of the work in the literature relies on the analysis, numerical and experimental validation, and on realistic applications as vibration absorbers in an audible frequency range and, therefore, they are well known as Acoustic Black Holes. One of the pioneers on ABHs is V.V. Krylov and co-workers [3,4,5,6]. Their results include one of the first industrial applications, by incorporating ABHs in the fins of a turbofan to reduce vibrations [4]. Other authors have obtained important theoretical results, looking for mathematical models different from the traditional ones based on the geometric acoustics approach [1,7,8]. With the advances and research on the subject, some possible applications have been proposed, such as some innovations on energy harvesters, to improve their efficiency by incorporating ABHs [3].

## III. Model of an ABH on an Euler-Bernoulli Beam

### A. Description of the beam with ABH

A beam-type ABH (see Fig. 1) consist in a secction change (thickness) along the longitudinal coordinate $x$, from $x_0$ till $x_{ANA}$, $x_0$ could be different to zero when truncation appears. The ABH length is $L_{ANA} = x_{ANA} - x_0$. The ABH profile has a maximum thickness in the $x_{ANA}$ coordinate and is equal with $h_0$. The section change is given by $h(x) = bx^k$ where $b$ is a constant coefficent and $k$ is an integer equal or greater than two. The last condition is necessary to get the phenomenon of vibration concentration, as described in [1,2].

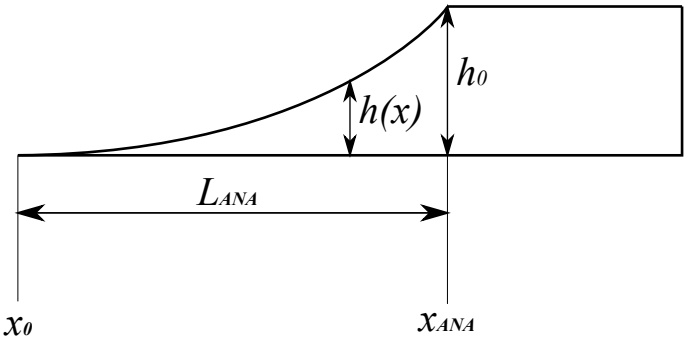


Fig. 1. Schematic diagram of a beam-type with an ABH part.

### B. Modeling a beam with ABH

The case study considers a Euler-Bernoulli beam, combining two parts: one segment with rectangular cross

section and other ending with an ABH, with a variable smooth reduction of its thickness up to a wedge-type profile (see Figs. 1 and 2). For modeling purposes, it is necessary to include both connected parts, using combined boundary conditions.

The equation of motion for a constant cross-sectional beam is described as [9-10]

$$\frac{\partial}{\partial^2}\left(EI\frac{\partial y}{\partial t^2}\right)+\rho A\frac{d^2y}{dt^2}=p(x,t) \quad (1)$$

where $y(x,t)$ represents the vertical displacements as a function of the spatial coordinate $x$ (length) and time $t$, and $E$, $\rho$, $I$ y $A$ are the Young's modulus of elasticity, material density, second moment of area and cross-sectional area, respectively. Here $p(x,t)$ denotes an external force, which for free vibration analysis $p(x,t)\equiv 0$.

In case of an ABH, $I$ and $A$ are no longer constant, which significantly alters equation (1). In fact, with a straight wedge profile with power-law thickness [1], results

$$x^{2k}\frac{\partial^4 y}{\partial x^4}+6kx^{2k-1}\frac{\partial^3 y}{\partial x^3}+3k(3k-1)x^{2k-2}\frac{\partial^2 y}{\partial x^2}-\alpha y=0 \quad (2)$$

where $\alpha$ is some constant, which depends on the material properties $E$ and $\rho$, frequency $\omega$ and specific shape of the beam tip. Moreover, the solution $y(x)$ strongly depends on the exponent $k$ corresponding to the ABH profile. For more details refer to [1-3].

### C. Specifications of the test specimen

To compare the phenomenon of a beam incorporating an ABH, the test specimen shown in Fig. 2 is considered. Its material properties and geometry are described in Table I. For evaluation purposes, the second test specimen is a uniform beam with constant cross section of the same material and dimensions.

Because the ABH exponent is set to $k=2$, then there is a case where (2) becomes a Cauchy-Euler equation, whose exact solution is of the form (see [1])

$$y(x)=x^{-\frac{3}{2}}\Big(c_1x^{-\frac{1}{2}\sqrt{17-4\sqrt{4+\alpha}}}+c_2x^{-\frac{1}{2}\sqrt{17-4\sqrt{4+\alpha}}} + c_3x^{\frac{1}{2}\sqrt{17+4\sqrt{4+\alpha}}}+c_4x^{\frac{1}{2}\sqrt{17+4\sqrt{4+\alpha}}}\Big) \quad (3)$$

where $c_i$, $i=1,\cdots,4$, are appropriate constants. This solution change it behavior in function of the frequency resulting in non-lineal motion at the tip with a stronger effect at high frequencies.

### D. Numerical results with a beam with ABH vs a uniform beam

The beam with ABH is a composition between a uniform beam with final end with ABH profile, such that, the complete model is obtained by coupling (1) and (3) through 4 continuity equations and 8 boundary conditions for both free extremes, in case of the uniform beam and that with ABH.

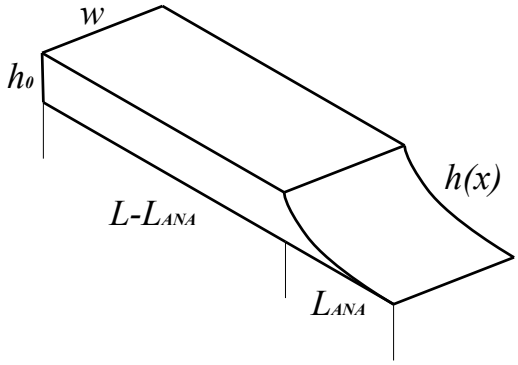


Fig. 2. Schematic diagram of a beam with an ABH at the tip wedge $h(x)$.

TABLE I
PARAMETERS OF BEAM WITH ABH.

| Specimen characteristics | |
|---|---|
| **Parameter** | **Value** |
| Material | AISI 1018 cold rolled |
| Young's modulus ($E$) | 200 GPa |
| Poisson ratio ($\nu$) | 0.266 |
| Isotropic losing factor ($\eta$) | 0.060 |
| Density ($\rho$) | 7860 kg/$m^3$ |
| Length (L) | 300 mm |
| wide (w) | 25.4 mm |
| thickness ($h_0$) | 6.3 mm |
| ABH exponent (k) | 2 |
| Second moment of area (I) | $5.2926\times10^{-10}$ $m^4$ |
| Cross sectional area (A) | 0.00016002 $m^2$ |
| ABH length ($L_{ANA}$) | 30 mm |

The beam was simulated with free ends and a lateral force of 1[N] was introduced at the free end of the ABH to determine the dynamic response to different frequencies. As a reference, the first 5 natural frequencies of the uniform beam are computed to know the behavior of the beam with ABH under similar conditions (see Table II). In addition, the first 5 vibration mode-shapes are shown in Fig. 3.

It is worth mentioning that, ABH have a cut-off frequency,from which the phenomenon of vibration concentration will occur. For the parameters in Table I, there is a cut-off frequency at 10.025 kHz (see, e.g., [3]). It was simulated with different frequencies, including those frequencies in Table II.

TABLE II
NATURAL FREQUENCIES OF A UNIFORM BEAM.

| Specimen characteristics | | | |
|---|---|---|---|
| **n** | $\lambda_n L$ | $\omega_n[rad/s]$ | $f_n[Hz]$ |
| 1 | 4.73 | 2280 | 362.96 |
| 2 | 7.8532 | 6286.41 | 1000.51 |
| 3 | 10.9956 | 12323.9 | 1961.5 |
| 4 | 14.1372 | 20372.2 | 3242.3 |
| 5 | 17.2788 | 30432.2 | 4843.44 |

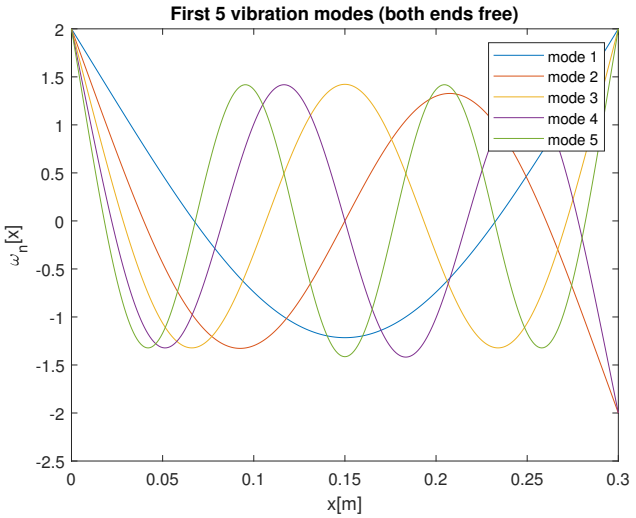


Fig. 3. Vibrations mode-shapes of a uniform beam.

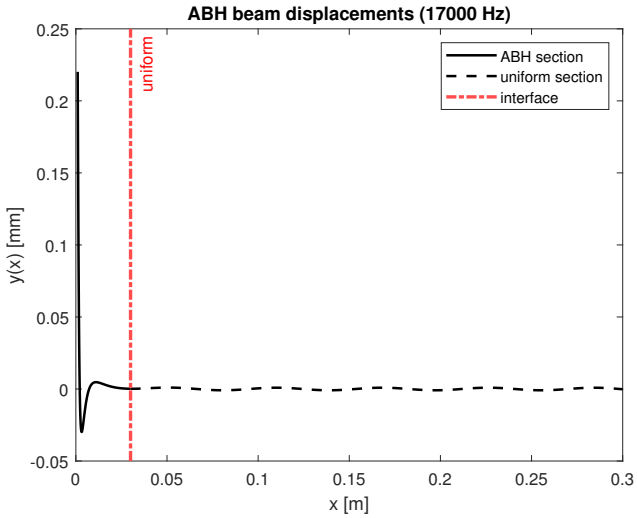


Fig. 5. Beam displacements with ABH at 17 kHz.

In Figs. 4 and 5 are shown the uniform part of the beam in dotted line (black) and then the part with ABH in solid line (black), both graphs depicts the phenomenon at frequencies of 1.21 kHz and 17 kHz, respectively. Note that, increasing the frequency also increases the effect of the ABH. In other words, the oscillations are concentrated in the ABH, and the uniform part vibrates with less amplitude.

On the other hand, the theoretical behavior is ideal, and corresponds to a thickness of zero at the tip of the ABH. However, a thickness of zero is physically impossible, since any manufacturing method will leave a small thickness, known as truncation. When considering such a truncation, the realistic behavior of the ABH significantly changes, leading to a less effective behavior, as can be observed by means of the reflection coefficient (shown in Fig. 6).

Thus, considering a truncation of 0.5 mm in the interval of 0 to 20 kHz, the best coefficient is greater than 0.84, which means that the ABH absorbs less than 20% of the vibrations.

To solve the problem of loss of efficiency on an ABH, some viscoelastic materials are incorporated, as will be shown in the next experimental results, which can improve the overall dynamic performance.

## IV. Experimental Validation

The specimens described in the previous Section were properly manufactured, and a first experiment consisting of obtaining the natural frequencies of the specimens from acceleration signals, generated by striking the specimens with an impact hammer was proposed. To simulate the free ends,

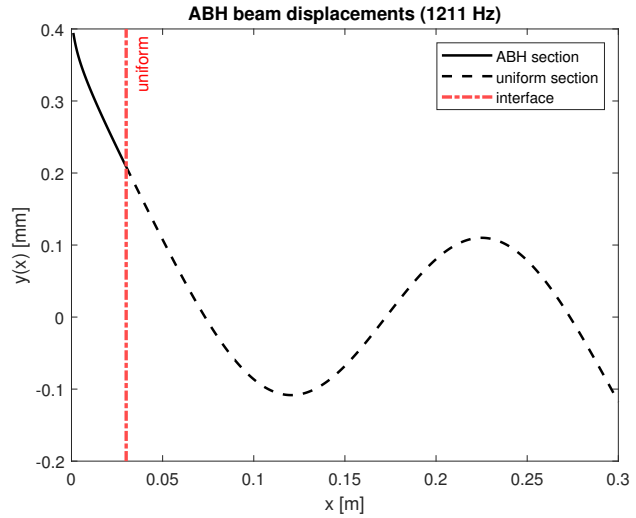


Fig. 4. Beam displacements with ABH at 1.21 kHz.

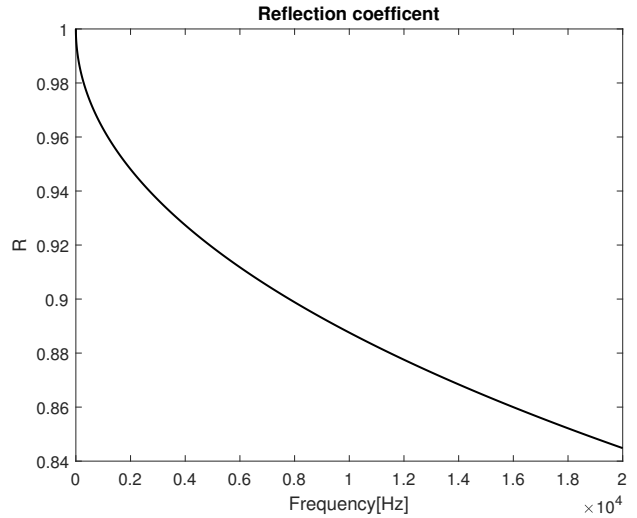


Fig. 6. Coefficient of reflection considering the truncation of 0.5 mm.

both specimens were suspended from long thin threads. As a second experiment, the audio on the specimens when they are hit, was captured to obtain a basic modal analysis and also some information on the signal attenuation. It is important to mention that, the experiments were carried out with four different cases: uniform, ABH, uniform with viscoelastic and ABH with viscoelastic strip. The viscoelastic material consists of just incorporating a rubber band at the tip of the specimens, as shown in Fig. 7. In the first experiment, only the natural frequencies were obtained in each case. For the second experiment, the natural frequencies were also calculated, and graphs of the audio signals were also obtained to compare the way in which the signals are dissipated. The results of both experiments are shown below.

### *A. Experiment 1.*

In this experiment an accelerometer with a sensitivity of 102 mV/g was used. Given the mode-shapes of Fig. 3 results convenient collocate the accelerometer in one of the free ends, specifically in the end without ABH and viscoelastic strip, this is to avoid add damping in the tip where viscoelastic strip or ABH are working. An unilateral spectrum was obtained from the acceleration signals to determine the natural frequencies of the first 5 vibrations modes reported in Table III.

TABLE III
NATURAL FREQUENCIES OBTAINED WITH ACCELEROMETER.

| Natural frequencies obtained from acceleration signal [Hz] | | | | |
|---|---|---|---|---|
| **n** | **uniform** | **ABH** | **uniform with viscoelastic** | **ABH with viscoelastic** |
| 1 | 368.19 | 416.27 | 367.23 | 415.03 |
| 2 | 1000.98 | 1123.84 | 1012.16 | 1122.50 |
| 3 | 1930.47 | 2146.52 | 1927.27 | 2138.40 |
| 4 | 3252.77 | 3463.57 | 3182.33 | 3447.27 |
| 5 | 4898.55 | 4854.35 | 4814.76 | 4866.54 |

Fig. 8 shows the dynamic response to the force applied by an impact hammer, with the acceleration in the beam and the unilateral spectrum of the acceleration signal for the case of a beam with ABH and viscoelastic strip.

### *B. Experiment 2.*

For this experiment the natural frequencies were also obtained for the four cases, shown in Table IV. It should be noted that, these frequencies were now obtained from an audio signal, captured by hitting specimens using a condenser microphone.

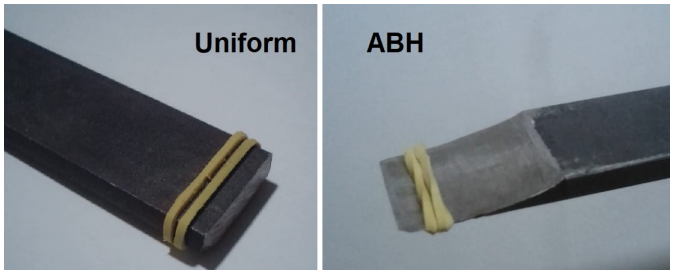


Fig. 7. Pictures of a uniform and ABH beams with viscoelastic (strip) material.

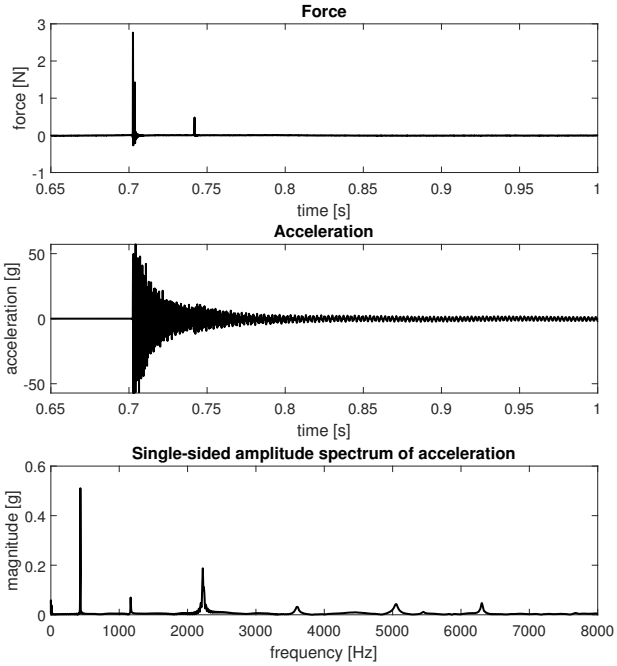


Fig. 8. Experiment 1: case of ABH with viscoelastic strip.

The audio signals are presented in Figs. 9 to 13. Fig. 9 shows the audio signals in the experiment without viscoelastic strip, the blue signal corresponds to the uniform beam and the black signal to the ABH. Fig. 10 shows the experiment with viscoelastic strip. Fig. 11 describes the comparison between the uniform beams with and without viscoelastic strip and Fig. 12 depicts the comparison between the ABHs with and without viscoelastic strip.

Finally, Fig. 13 describes the main differences between a uniform beam without viscoelastic and an ABH with viscoelastic, clearly with a notorious difference, quantified in the next section.

TABLE IV
NATURAL FREQUENCIES OBTAINED BY AUDIO.

| Natural frequencies obtained from audio signal [Hz] | | | | |
|---|---|---|---|---|
| **n** | **uniform** | **ABH** | **uniform with viscoelastic** | **ABH with viscoelastic** |
| 1 | 364.13 | 418.41 | 363.28 | 417.23 |
| 2 | 1001.96 | 1141.29 | 1001.11 | 1139.53 |
| 3 | 1961.13 | 2204.17 | 1958.66 | 2198.29 |
| 4 | 3223.66 | 3543.74 | 3222.98 | 3529.38 |
| 5 | 4875.72 | 5229.12 | 4792.21 | 4879.46 |

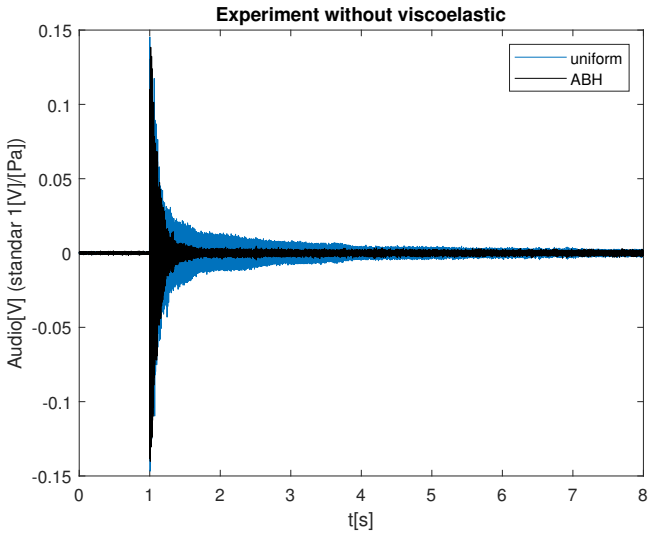


Fig. 9. Experiment 2: beams uniform and ABH without viscoelastic strip.

## V. Results and Discussion

In Figs. 9 to 13 there is a faster energy dissipation when a viscoelastic, an ABH or both are included. Thus, to obtain a quantitative measure of such a dissipation, it was determined as the setting level of the audio signal an amplitude of $2 \times 10^3$, which corresponds mainly to high-frequency noise, from this it is possible to measure the times that the signals take to establish themselves.

The establishment times are shown in Table V, considering as 100% the time it takes to establish the signal of the uniform beam. In addition to the experimental results, the errors were calculated between natural frequencies obtained for experiments 1 and 2, with respect to the theoretical natural frequencies in Table II (see also Table VI).

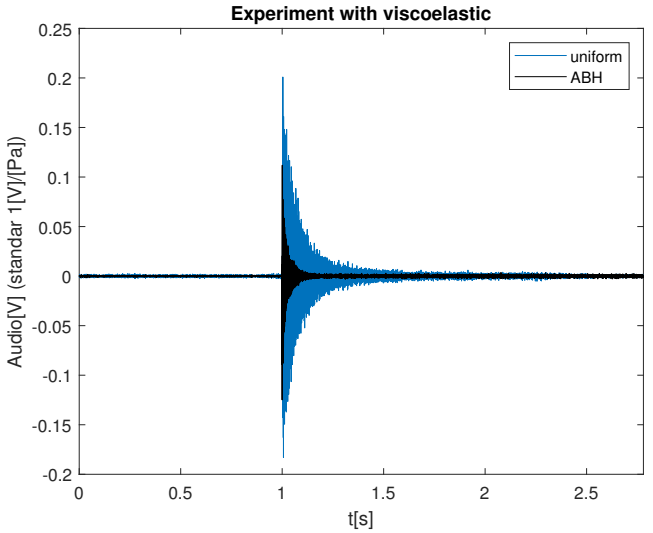


Fig. 10. Experiment 2: beams uniform and ABH with viscoelastic strip.

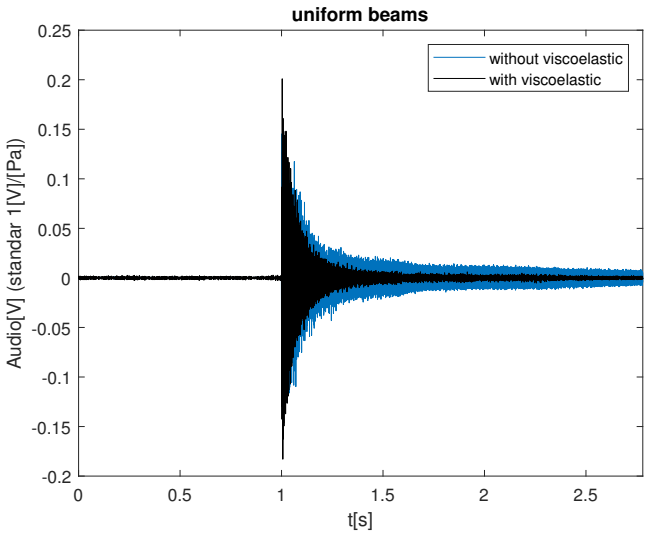


Fig. 11. Experiment 2: uniform beam with and without viscoelastic strip.

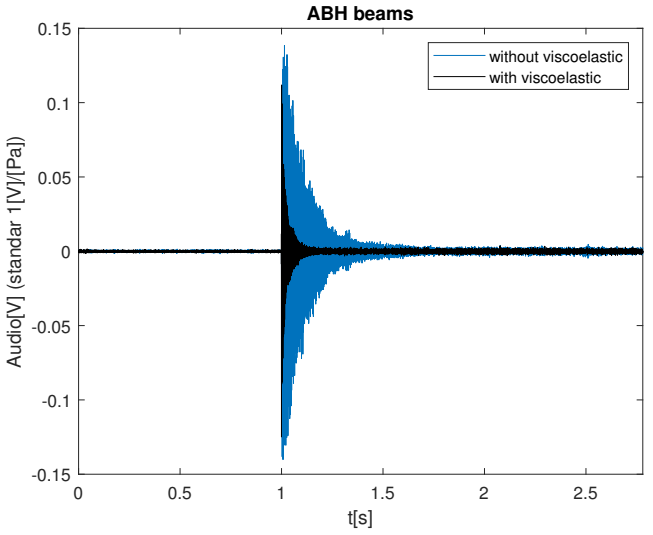


Fig. 12. Experiment 2: ABH beam with and without viscoelastic strip.

TABLE V
Settling Time Evaluation.

| Experimental Settling times | | |
|---|---|---|
| **Beam type (specimen)** | **Settling time [s]** | **%** |
| Uniform | 7.45 | 100 |
| ABH | 1.84 | 25 |
| Uniform with viscoelastic strip | 2.44 | 33 |
| ABH with viscoelastic strip | 1.26 | 17 |

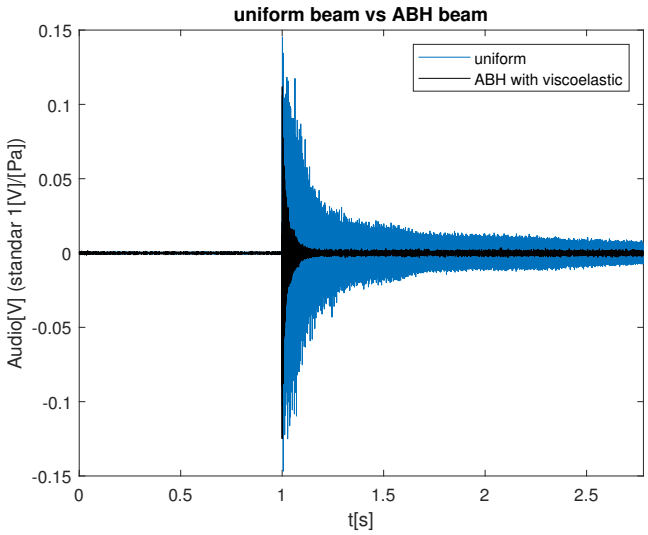


Fig. 13. Experiment 2: uniform beam without viscoelastic strip and ABH with viscoelastic strip.

With the experiments carried out, the phenomenon of an ABH was clearly validated, that is, how they concentrate and dissipate vibrations more quickly (about 4 times faster than the uniform beam). In addition, the increase in the effectiveness of an ABH was verified by incorporating a viscoelastic material, dissipating vibrations almost 6 times faster with respect to a uniform beam without the viscoelastic strip.

It is important to note that, experiment 2 was a low-cost compared to experiment 1, but still providing accurate information as shown by the errors in Table VI. Then, it is feasible to integrate an acoustic measurements system as an alternative to perform basic modal analysis on this type of mechanical structures. Some important considerations, when applying acoustical methods for vibration measurements, are the following: Microphone location. It is important to position the microphone to directly capture the vibrations in the direction of interest, and not to capture vibrations on other directions or vibration modes. This is achieved by adequately placing the microphone parallel to the plane of interest. Environmental noises. As it is audio, then it is possible to capture measurements with environmental noise. Thus, two signal processing to this problem can be to filter the signal or, alternatively, to carry out the test in places isolated from noise.

TABLE VI
ESTIMATION ERROR ON NATURAL FREQUENCIES

| **% Error in the natural frequencies obtained by audio and acceleration** | | |
|---|---|---|
| **Vibration mode** | **%Error experiment 1** | **%Error experiment 2** |
| 1 | 1.4409 | 0.03223 |
| 2 | 0.0469 | 0.1449 |
| 3 | 1.5819 | 0.0188 |
| 4 | 0.3229 | 0.5749 |
| 5 | 1.1378 | 0.6664 |

## VI. CONCLUSIONS

Regarding the application of the ABHs as passive vibration absorbers, the results of the experiments are encouraging to continue analyzing and testing with other types of structures. More realistic applications of the ABHs, under this approach, can be implemented as solutions for acoustic and/or vibration attenuation. This implies that some components of mechanical structures could have an integrated passive vibration absorbers in it self geometry with the aim to reduce noise. The experiments are simple but effective to validate the ABH phenomenon, and show how incorporating an ABH of power-law of two and a viscoelastic strip at the end of a beam the settling time is reduced to 17% regarding to uniform beam. Thus through structure analysis and appropriate tuning of ABH cut-off frequency there is a possibility to get reduced the noise and vibrations in mechanical structures. Besides, exist other types of ABH's that work under the same physical principles and allow be integrated in different geometries like plates, shafts and so on opening the application possibilities.

## REFERENCES

[1] J. Y. Lee and W. Jeon, "Exact solution of euler-bernoulli equation for acoustic black holes via generalized hypergeometric differential equation," *Journal of Sound and Vibration*, vol. 452, pp. 191–204, 2019.
[2] V. V. Krylov, "Acoustic black holes for flexural waves: A smart approach to vibration damping," *Procedia Engineering*, vol. 199, pp. 56–61, 2017. X International Conference on Structural Dynamics, EURODYN 2017.
[3] A. Pelat, F. Gautier, S. C. Conlon, and F. Semperlotti, "The acoustic black hole: A review of theory and applications," *Journal of Sound and Vibration*, vol. 476, p. 115316, 2020.
[4] E. Bowyer and V. Krylov, "Damping of flexural vibrations in turbofan blades using the acoustic black hole effect," *Applied Acoustics*, vol. 76, pp. 359–365, 2014.
[5] V. Krylov and F. Tilman, "Acoustic 'black holes' for flexural waves as effective vibration dampers," *Journal of Sound and Vibration*, vol. 274, no. 3, pp. 605–619, 2004.
[6] V. Krylov and R. Winward, "Experimental investigation of the acoustic black hole effect for flexural waves in tapered plates," *Journal of Sound and Vibration*, vol. 300, no. 1, pp. 43–49, 2007.
[7] L. Tang, L. Cheng, H. Ji, and J. Qiu, "Characterization of acoustic black hole effect using a one-dimensional fully-coupled and wavelet-decomposed semi-analytical model," *Journal of Sound and Vibration*, vol. 374, pp. 172–184, 2016.
[8] L. Tang and L. Cheng, "Enhanced acoustic black hole effect in beams with a modified thickness profile and extended platform," *Journal of Sound and Vibration*, vol. 391, pp. 116–126, 2017.
[9] W. T. Thomson and M. D. Dahleh, *Theory of vibrations with applications*. Pearson, 2014.
[10] S. S. Rao, *Vibraciones Mecanicas*. Pearson, 2012.